HHS Public Access

Author manuscript

Microcirculation. Author manuscript; available in PMC 2016 February 01.

Published in final edited form as:

Microcirculation. 2015 February ; 22(2): 109–121. doi:10.1111/micc.12183.

Heterogeneity in Kv7 channel function in the Cerebral and Coronary Circulation

Sewon Lee[#1], **Yan Yang**[#1], **Miles A. Tanner**[1], **Min Li**[1], and **Michael A. Hill**[1,2]

[1]Dalton Cardiovascular Research Center, University of Missouri-Columbia, MO 65211

[2]Department of Medical Pharmacology & Physiology, University of Missouri-Columbia, MO 65211

[#] These authors contributed equally to this work.

Abstract

Kv7 channels are considered important regulators of vascular smooth muscle contractility. The present study examined the hypotheses that 1. Kv7 channels are present in mouse cerebral and coronary arteries and regulate vascular reactivity, and 2. regional differences exist in the activity of these channels. PCR confirmed that basilar, Circle of Willis and left anterior descending (LAD) arteries express predominantly Kv7.1 and 7.4. Western blot analysis, however, showed greater Kv7.4 protein levels in the cerebral vessels. Relaxation to the Kv7 channel activator, retigabine (1-50μM) was significantly greater in basilar compared to LAD. Similarly, the Kv7 channel inhibitor, linopirdine (10μM) caused stronger contraction of the basilar artery. Furthermore, pre-incubation with linopirdine reduced forskolin (cAMP activator)-induced vasorelaxation in basilar while not altering forskolin-induced vasorelaxation of the LAD, suggesting that Kv7 channels play a more prominent role in the cerebral than coronary circulation. Consistent with the vessel data, whole cell Kv7 currents in cerebral VSMCs were potentiated by retigabine and inhibited by linopirdine, while these responses were blunted in coronary VSMCs. This study provides evidence that mouse Kv7 channels may contribute differently to regulating the functional properties of cerebral and coronary arteries. Such heterogeneity has important implications for developing novel therapeutics for cardiovascular dysfunction.

Keywords

K^+ channels; voltage-gated K^+ channels; cerebral and coronary arteries; regional heterogeneity; electrophysiology; pharmacological manipulation

1. INTRODUCTION

Increasing intralumenal pressure or the application of vasoconstricting agonists typically leads to vascular smooth muscle cell (VSMC) depolarization, activation of ion channels including voltage-dependent Ca^{2+} channels, Ca^{2+} mobilization and vascular constriction

Correspondence: Michael A. Hill, PhD, Dalton Cardiovascular Research Center, University of Missouri, 134 Research Park Drive, Columbia, Missouri 65211, USA, Hillmi@missouri.edu.

Disclosures
None.

[1,2]. Membrane potential is tightly regulated by K^+ channels expressed in VSMCs and malfunction of these channels may result in pathophysiological conditions such as vasospasm as well as an impaired ability to vasodilate and lower vascular resistance [2-4]. VSMCs express a number of distinct types of K^+ channels including large conductance Ca^{2+} activated K^+ (BK_{Ca}), ATP-sensitive K^+ (K_{ATP}), inward rectifier K^+ (K_{ir}), two pore domain K^+ (K_{2p}) and voltage-gated K^+ (Kv) channels [2-5]. Amongst these various channels, Kv channels are widely expressed in VSMCs and postulated to be critical regulators of both vascular tone and resting membrane potential [5,6]. Importantly, and directly relevant to the current study, various Kv channels have been shown to play an important role in the regulation of coronary blood flow [7-9] as well as small cerebral artery myogenic tone [10-12]. There are several subtypes of Kv channels and it is known that Kv7 channels encoded by *KCNQ* gene family are expressed in various arteries of a number of species including mouse, rat, pig and human [10,13-20]. In addition, recent studies have implicated Kv7 channels as important regulators of smooth muscle contractility in the vasculature including in aorta, renal, coronary and cerebral arteries [10,13,15,16,18]. Even though these channels are widely expressed in mammalian vascular smooth muscle, it is not clear that Kv7 channels regulate the same functions in different vascular beds and, if so, whether efficacy is similar across these regions.

Heterogeneity in regard to Kv7 function, between cerebral and coronary vascular beds, may result in differences in response to Kv7 modulators. On the basis of the above considerations, the present study was undertaken to 1. Study whether Kv7 channels are present in mouse cerebral and coronary arteries and their contribution to modulating vascular reactivity and 2. Compare the pharmacological and electrophysiological properties of Kv7 between cerebral and coronary arteries. Demonstration of involvement of specific Kv7 subtypes potentially provides the rationale for specific pharmacological intervention in different vascular beds. Further, understanding tissue selectivity (for example cerebral vs. coronary artery) may provide the potential for targeting specific vascular complications such as cerebrovascular and coronary dysfunction.

Materials and Methods

Animal Procedures

All experimental protocols were approved by the Animal Care and Use Committee of the University of Missouri (USA). Eighteen to twenty two-week old male WT mice (Background Strain: C57BLKS/J) were used in this study. Mice were housed in a temperature-, humidity-, and light-controlled animal facility and provided with free access to standard mouse chow and water. Mice were anaesthetized with sodium pentobarbital (Nembutal, 100 mg kg body weight^{-1}) given by intraperitoneal injection. The heart was surgically removed and placed in cold physiological saline solution (PSS) containing (in mM): NaCl, 140; KCl, 4.7; $MgSO_4 \cdot 7H_2O$, 1.17; $NaH_2PO_4 \cdot H_2O$, 1.2; $CaCl_2 \cdot 2H_2O$, 2.0; D-glucose, 5.0; pyruvic acid, 2.0; EDTA, 0.02; MOPS, 3.0; plus 10 mg ml^{-1} BSA (USB Corporation, Cleveland, OH, USA). Following death by heart removal, a craniotomy was performed, and the brain was removed and similarly placed in a cooled dissection chamber as above.

Functional assessment of cerebral and coronary arteries

Basilar and proximal left anterior descending (LAD) arteries were exposed from the brain and heart respectively and microdissected in the cold chamber (4°C). Vessel ring segments (endothelium intact) of 1.5-2 mm in length were transferred to the myograph (Danish Myo Technology, Model 610, Aarhus, Denmark) chamber with PSS containing (in mM): NaCl, 118.99; KCl, 4.69; KH_2PO_4, 1.18; $MgSO_4 \cdot 7H_2O$, 1.17; $CaCl_2 \cdot 2H_2O$, 2.5; $NaHCO_3$, 25; D-glucose, 5.5; EDTA, 0.03 and mounted using two 25 μm stainless wires. Vasoreactivity was assessed under isometric conditions and responses were recorded using a PowerLab system (AD instruments, CO, USA). After a 30-min equilibration period, both artery types were placed under a tension equivalent to 90% of the diameter of the vessel at a transmural pressure of 100 mm Hg [21]. Then, 30 min of equilibration was allowed. All vessels were stimulated with cumulative addition of high K^+ (30-120 mM KCl) to assess viability (Supplementary figure 1A). In some experiments, U-46619 (Thromboxane A_2 receptor agonist) dose-response curves were examined in both basilar and LAD arteries (Supplementary figure 1B). Based on these preliminary studies, both arteries were first pre-contracted with 100 nM U-46619 for 10-15 min to provide a stable level of basal tone so as vasorelaxation could be determined. After a sustained contraction was evoked, concentration-response curves were obtained by a cumulative addition of the Kv7 activator, retigabine (1 - 50 μM). Relaxation at each concentration was measured and expressed as the percentage of force generated in response to U-46619. The inhibitory contributions of Kv7 channels to vasorelaxation or vasoconstriction were assessed by pre-incubating arteries with the non-selective, pan Kv7 channel blockers, linopirdine (10 μM) or XE991 (10 μM). The vessels were subsequently pre-constricted with 100 nM U-46619 and relaxation was measured by cumulative addition of the cAMP activator, forskolin (1 nM-1 μM). All vessels were maintained in PSS gassed (95% O_2 and 5% CO_2) to maintain pH (7.4) at 37°C for the entire experiment.

Electrophysiological recordings (Patch clamp)

Cerebral arteries were dissected from the Circle of Willis and the LAD excised from the heart as above. Cerebral arteries were then enzymatically digested in a two-step process to isolate single VSMCs as outlined in previous studies of a rat model [22]. In detail, cerebral artery segments were transferred to 0.1 mM Ca^{2+} PSS (1 ml) containing (in mM): NaCl, 144; KCl, 5.6; $CaCl_2$, 0.1; $MgCl_2$, 1.0; Na_2HPO_4, 0.42; HEPES, 10; sodium pyruvate, 2; and 1 mg ml^{-1} BSA at room temperature for 5 min. Step 1: the solution was decanted and replaced with a similar solution containing 26 U ml^{-1} papain and 1 mg ml^{-1} dithiothreitol (DTT). The vessels were then incubated for 10 min at 37°C with occasional agitation, following by washing 2-3 times in enzyme free low Ca^{2+} PSS. Step 2: 1.95 U ml^{-1} collagenase (Type H FALGPA), 0.4 mg ml^{-1} type F collagenase in 0.1 mM Ca^{2+} PSS was used for 2-3 min to further digest the vessels. After washing 2-3 times, the vessels were triturated with a fire-polished glass pipette and the liberated VSMCs stored in ice-cold PSS for use within 4 hrs. The method for isolation of cells from the LAD artery was similar to that used previously [22]. Briefly, LAD segments were bathed in 0.1 mM PSS for 5 min and exposed to papain and DTT for 15 min. After washing 2-3 times, the LAD arteries were incubated with 0.1 mM PSS containing 1.95 U ml^{-1} collagenase (Type H FALGPA), 1 mg ml^{-1} soybean trypsin inhibitor and 75 U ml^{-1} elastase for 4-5 min at 37°C. The fragments

were then washed 2-3 times and triturated with a fire-polished glass pipette to release single cells. Control experiments have previously been performed to ensure that the procedures, *per se*, did not introduce differences in electrophysiological responses [23].

Conventional patch-clamp electrophysiology [24] and protocols were used to measure macroscopic whole-cell K^+ currents from both cerebral and LAD artery smooth muscle cells (SMCs). All experiments were performed at room temperature. An amplifier (EPC-10, HEKA, Germany) was controlled by a Dell computer using Patchmaster and Igor Pro 6.11 (Wavemetrics, Inc., Lake Oswego, OR, USA). Micropipettes were pulled from borosilicate glass tubing (Corning 8161; i.d. 1.2 mm; o.d. 1.5 mm; Warner Instruments Corp., Hamden, CT, USA) using a Sutter P-97 electrode puller (Sutter Instrument Co., Novato, CA, USA). Pipette tip resistances ranged from 3.0 to 5.0 MΩ when filled with standard intracellular solution. Whole-cell K^+ currents were evoked by voltage steps delivered from a holding potential of −70 mV to potentials ranging from −70 to +70 mV, in 20 mV increments. Cell capacitance was measured with the cancellation circuitry in the voltage-clamp amplifier. Series resistance (<10 MΩ) was compensated to minimize the duration of the capacitive surge. Subtraction of leak currents was not performed. Whole-cell currents were normalized to cell capacitance and expressed as picoampere per picofarad ($pA \cdot pF^{-1}$). For whole-cell recordings, the bath solution contained (in mM): NaCl, 140; KCl, 5.4; $CaCl_2$, 1; $MgCl_2$, 1; glucose, 10; HEPES, 10; sodium pyruvate, 2 (pH 7.4). The 140 mm K^+ pipette solution contained (in mM): KCl, 140; NaCl, 8; EGTA, 10; Mg-ATP, 3; HEPES, 10; GTP, 1 (pH 7.2); $CaCl_2$ was added to bring free $[Ca^{2+}]$ to 300 nm. The presence of Kv7 currents was inferred by the existence of a linopirdine- or XE991- sensitive component of total K^+ current. 4-AP and paxilline were used to inhibit Kv currents and BK_{Ca} current, respectively. Mg-ATP was included to inhibit ATP- sensitive K^+ channels and provide substrate for energy-dependent processes. Where addition of other reagents to the bath and/or pipette solutions was required, details are given in specific protocols and figure legends.

End-point and quantitative PCR

Total RNA was extracted from cerebral and coronary arteries using the Arcturus PicoPure RNA isolation kit (Applied Biosystems, Carlsbad, CA) with on-column DNase I treatment (Qiagen, Valencia, CA) according to the manufacturer's instructions. RNA was eluted with 25 μl nuclease-free water. Using random hexamer and oligo d(T) primers, 8 μl of eluted RNA was subjected to reverse-transcription into cDNA using the SuperScript III First-Strand Synthesis System (Life Technologies, Grand Island, NY) in a final volume of 20 μl. End-point PCR was first carried out to detect expression of Kv7 channel subtypes in basilar, LAD artery, heart and brain. All PCR reactions (25 μl) contained 1 μl of first-strand cDNA mixture as template, 3 mM $MgCl_2$, 0.25 μM primers, 0.2 mM deoxynucleotide triphosphates; and GoTaq Flexi DNA polymerase (Promega, Madison, WI). The PCR program was comprised of an initial denaturation step at 95°C for 2 min; followed by 35 cycles of denaturation for 20 sec at 95°C, annealing 30 sec at 60°C, and elongation for 30 sec at 72°C; and a final extension step at 72°C for 5 min. Primers in this study were based on results published previously [13]. The expected size of PCR products and primer sequences are listed in Table 1. PCR amplification products were separated on a 2 % agarose gel by electrophoresis and the DNA bands were visualized by ethidium bromide

staining. Quantitative PCR (qPCR) was performed using the SYBR® Green chemistry with an iQ5 iCycler (Bio-Rad Laboratories, Hercules, CA). The qPCR primers used for Kv7 channels were predesigned and purchased from Integrated DNA Technologies (Coralville, IA). 18S rRNA was used as a reference gene and internal standard [25-27]. Sequences for all qPCR primers are provided in Table 2. All qPCR reactions were prepared in a volume of 25 μl with final concentrations of 1 × Platinum® SYBR® Green qPCR SuperMix-UDG (Life Technologies, Grand Island, NY), 0.5 μM primer and 1 μl of first-strand cDNA reaction. Thermal cycling conditions for qPCR comprised an initial UDG incubation at 50°C for 2 min, polymerase activation at 95°C for 2 min, 40 cycles of denaturation at 95°C for 10 sec, annealing and extension at 57°C for 30 sec. A melting curve was generated after each run to ensure the specificity of the amplified products. Relative expression levels were assessed using the comparative threshold (Ct) values according to the $2^{-\Delta\Delta Ct}$ method [28].

Western Blot Analysis

Basilar, proximal left anterior descending (LAD) arteries and cerebral arteries from the Circle of Willis were dissected as described above (n = 7 animals). In the case of basilar arteries, vessels were pooled from two animals to generate one sample. Vessels were homogenized for protein extraction as previously described [22]. Approximately equal amounts of total protein were loaded onto 8% SDS-PAGE gels, separated by electrophoresis and then transferred onto a PVDF membrane (Bio-Rad). The membranes were first probed with anti-Kv7.4 antibody (1:300; Santa Cruz, sc-50417) and anti-rabbit horseradish peroxidase conjugated secondary antibody (1:8000; Life Technologies, 65-6120). The membranes were then incubated with anti-(pan) actin antibody (1:2000; Cytoskeleton, AAN01) to determine protein loading. Chemiluminescence signals were detected by Bio-Rad Chemi-DOC XRS+ digital system and band intensities were quantified using ImageLab software (Bio-Rad, Hercules, CA, USA). The expression level of Kv7.4 was normalized to actin.

Statistical Analysis

All values were presented as means ± SEM. Student t-tests were used where the means of two groups were compared. Comparisons of multiple groups were performed using ANOVA Bonferroni's post-hoc testing. Statistical differences were accepted at the $p<0.05$ probability level unless otherwise stated. All statistical analyses were performed using either Prism 5 or SigmaPlot 12.

Chemicals

Unless stated, general chemicals and reagents were purchased from Sigma-Aldrich (St Louis, MO, USA). Retigabine were purchased from Sigma-Aldrich and Medchem Express (Princeton, NJ, USA). Linopirdine, XE991, paxilline, TEA, 4-AP, forskolin, NS-1619 and U-46619 were purchased from Sigma-Aldrich. Retigabine (50 mM), XE991 (20 mM), paxilline (10 mM) and forskolin (5 mM) was dissolved in DMSO, while linopirdine (10 mM), NS-1619 (50 mM) and U-46619 (1 mM) stock solutions were made in ethanol. Appropriate vehicle control experiments were performed.

3. RESULTS

Expression of Kv7 subtypes in coronary and cerebral artery

To determine the expression profile of *KCNQ* genes in cerebral and coronary arteries, we first performed end-point PCR. Consistent with previous studies [10,13,15], our results (Figure 1A) show that *KCNQ* 1 (Kv7.1) and *KCNQ* 4 (Kv7.4) to be the predominant subtypes expressed in basilar and LAD arteries. However, expression of *KCNQ* 2,3 and 5 mRNA appeared comparatively low both in basilar and LAD arteries even though these subtypes were highly expressed in mouse brain (Figure 1A). Quantitative analysis of the relative abundance of Kv7.1 through 5 mRNA was performed on cerebral (basilar and Circle of Willis) and coronary (LAD) arteries. Consistent with the end-point PCR results, Kv7.1 and Kv7.4 were expressed at higher levels compared to Kv7. 2, 3 and 5 in both cerebral and coronary arteries (Figure 1B-D and Supplementary Figure 1C). To allow comparison of mRNA levels for a particular Kv7 channel protein, real time PCR data was plotted as a normalized ratio (relative to 18S mRNA levels; Supplementary Figure 1C). The data again emphasize the predominant expression of Kv7.1 and 7.4 in each of the vessel studied. mRNA expression for Kv7.1 and 7.4 was greater in basilar artery compared to either Circle of Willis arteries or the LAD. No significant differences were observed in expression levels between Circle of Willis arteries and the LAD.

To examine protein expression levels, Western blot studies were performed for Kv7.4 in basilar arteries, the Circle of Willis and the LAD (Figure 1E). Kv7.4 ran as an approximately 73 kD protein consistent with previous reports [29,30]. Kv7.4 levels (normalized to actin content) were found to be significantly lower in LAD compared to either of the cerebral vessel preparations (Figure 1E).

Effect of Kv7 channel modulators on cerebral and coronary reactivity

The functional contribution of Kv7 channels in the cerebral and coronary vessels was assessed with the Kv7 channel activator, retigabine. Figure 2 shows that retigabine induced a concentration-dependent vasorelaxation (10 - 50 μM) in the cerebral arteries, while this response was comparatively less in the coronary arteries. These data suggest that the Kv7 channel activator is a more effective relaxant of U-46619-preconstricted mouse cerebral arteries compared to the LAD.

Kv7 agonists such as retigabine hyperpolarize VSMCs and induce vasorelaxation, whereas non-selective Kv7 channel inhibitors (Kv7.1 through Kv7.5), linopirdine and XE991 have a depolarizing effect on VSMCs, causing contraction in renal, pulmonary, cerebral, mesenteric arteries and aorta [13,15,18,31,32]. Figures 3A and B show that application of 10 μM of linopirdine- or XE991 induced constriction of the cerebral artery while linopirdine-induced constriction was less in magnitude compared to that in the LAD. Linopirdine-induced constriction was relatively smaller than either TEA (1 mM)- or 4-AP (1 mM)-induced constriction both in cerebral and coronary arteries (Supplementary Figure 2A and B) suggesting that Kv7 component was a relatively small component of the overall K^+ conductance. Figures 4A and B show that the cAMP activator, forskolin induced a concentration-dependent relaxation in both mouse coronary and cerebral arteries. The

forskolin-induced vasorelaxation was attenuated by pre-incubation of cerebral arteries with 10 μM linopirdine, while linopirdine did not alter the vasorelaxation in coronary artery. Taken together, these data support Kv7 channel modulators being more effective in the cerebral circulation in comparison to the coronary circulation.

Dominance of the presence of Kv7 currents in freshly isolated cerebral myocytes

In earlier studies, we and others have shown an important role for Kv and BK_{Ca} channels in VSMCs from rat small arteries [2,23,33] while Zhong et al. suggested a role for Kv7 channels in regulating myogenic tone of rat cerebral arteries [10]. To determine whether Kv7 channels are present and modulate K^+ current in SMCs from mouse cerebral and coronary arteries, we similarly performed whole cell K^+ current recordings from isolated myocytes using the patch-clamp technique. Kv channel and BK_{Ca} channels were blocked by 4-AP (1 mM) and paxilline (20 μM) respectively, and XE991 (10 μM) was added sequentially to inhibit Kv7 channel currents in cerebral arteries, if present. Each of these inhibitors exert individual effects on cerebral SMC K^+ currents; specifically XE991 inhibited a small residual of component (~20%) of the total K^+ current amplitude (Supplementary Figure 3A-C) consistent with the vessel data described above. In isolated coronary artery myocytes, 4-AP and paxilline caused additive inhibition of the outward K^+ current, while XE991 had less of an effect relative to that in cerebral artery SMCs (Supplementary Figure 4A-C).

Because we found pharmacological evidence for Kv7 channel currents being present in cerebral artery SMCs, we determined whether activation of the Kv7 channels would increase outward K^+ current. Consistent with previous reports [34,35], retigabine (20 μM), a selective Kv7 channel (Kv7.2-7.5) activator, significantly enhanced the K^+ current over the voltage range +10 mV to +70 mV. The enhanced outward current was inhibited by 10 μM linopirdine (Figure 5A-D).

To determine whether inhibiting Kv7 channels in cerebral myocytes alters basal Kv currents, we first added linopirdine followed by retigabine. The outward Kv7 currents from cerebral artery myocytes were inhibited by linopirdine (10 μM), whereas the Kv7 channel activator retigabine (20 μM) could not reverse the effect of linopirdine (Figure 6A-D). In the coronary artery myocytes, the Kv7 channel activator retigabine did not increase K^+ current over the voltage range of -70 mV to +70 mV (Figure 7A-C). Under basal recording conditions in coronary myocytes, linopirdine showed minimal inhibition of Kv7 while sequential addition of retigabine did not potentiate K^+ currents (Figure 7D and E).

Analysis of biophysical characteristics of the channel recordings further supported Kv7 channels being more dominant in the cerebral vessels compared to the LAD. Estimated reversal potentials (E_{Rev}) showed that in cerebral VSMCs retigabine caused a small hyperpolarization (approximately 3.5 mV) while linopirdine treatment resulted in depolarization (approximately 4 mV) (Table 3). Similar shifts in E_{Rev} were not apparent for the VSMCs from LAD (Table 3). Calculation of normalized conductance (G/Gmax) curves similarly showed VSMCs from cerebral vessels to be modulated by retigabine (Figure 5C and D) and linopirdine (Figure 6C and D) as indicated by significant differences in the voltage for half maximal activation ($V_{1/2}$) (Table 3). Similar effects were not detected in

VSMCs from LAD (Figure 7C and E). The significant shifts in conductance induced by the Kv7 channel modulators in the cerebral VSMCs allowed calculation of drug sensitive or difference curves (Figures 5D and 6D) and a considerably left-shifted $V_{1/2}$ (Table 3).

4. Discussion

Smooth muscle Kv7 channels have been implicated as significantly contributing to the control of vascular reactivity and vasorelaxant responses [10,15,35]. To date, 5 subtypes of Kv7 channels encoded by *KCNQ* genes have been identified [36]. Previously, we have shown heterogeneity in ion channel subunit expression between vascular beds with emphasis on differences in the molecular composition and role of BK_{Ca} channels between cerebral and cremaster muscle vascular beds [23,37]. Little is known, however, as to differences in the role of Kv7 channels between the cerebral and coronary vasculature, despite these both being vital organs and sites contributing to the morbidity and mortality associated with cardiovascular disease. In the cerebral circulation, arteries such as basilar and those of the Circle of Willis exhibit a significant component of vascular resistance, making them important regulators of cerebral blood flow [38]. Further, the LAD artery plays a major role in the supply of blood to the heart and is the most commonly occluded coronary artery in coronary vascular disease [39]. Thus, delineating the cellular mechanisms regulating blood flow at the local level is important to both understanding vascular heterogeneity and potential identifying sites for novel and specific modes of pharmacological intervention.

Both end-point and qPCR showed that Kv7.1 and Kv7.4 to be the predominant Kv7 channel subtypes expressed in the cerebral and coronary arteries (Figure 1). Interestingly, studies have recently shown that Kv7.5 was relatively expressed high in rat cerebral and mesenteric arteries and that Kv7.5 forms a dimer with Kv7.4 in functional channels [29,30]. Our results, however, suggest that Kv7.5 expression is in fact comparatively low both in basilar and LAD from WT mice. This may reflect differences between species or heterogeneity between vascular beds although a caveat relates to our data being limited to expression at the mRNA level. Interestingly, we were able to detect Kv7.5 by PCR in brain and heart tissue indicating that the primers used were capable of detecting the transcript. Also supporting the validity of our findings in the mouse, PCR primer efficiencies were similar allowing comparison of relative expression levels of the various Kv7 transcripts to be made (Table 2). As this has potential implications for the molecular composition of the functional channel in mouse tissues, further studies are required.

An additional finding in the expression data was that mRNA levels for the various Kv7 channel proteins may also vary within a vascular bed. Specifically, Kv7.1 and 7.4 were found to be greater in the basilar artery compared to arteries taken from the Circle of Willis (Supplementary Figure 1C). Thus, this suggests heterogeneity in ion channel expression between branch orders within a vascular bed. Further supporting this, Plane et al. [33] previously showed that Kv1 mRNA expression levels to vary between branch orders of the mesenteric vascular beds. In that study, Kv1 mRNA levels were significantly greater in first order as compared to the smaller fourth order branches [33]. Despite the significant expression of Kv7.1 and Kv7.4 mRNA in the coronary arteries, retigabine-induced vasorelaxation was attenuated compared to that of cerebral artery (Figure 2). According to

previous studies, retigabine increases Kv7.2 through 7.5-mediated K^+ currents but not Kv7.1, which lacks the tryptophan residue within the S5 segment requiring for the sensitivity of retigabine [31,34,40,41]. Thus, based on pharmacological studies in conjunction with measurements of vasoreactivity in the cerebral vasculature appears to have an enhanced role for Kv7.4 as compared to the coronary vascular beds. Further, the effects of linopirdine are consistent with basal Kv7 channel activity in the cerebral VSMCs while this is minimal in the smooth muscle cells from LAD.

An additional two lines of evidence supported the functional data. Firstly, measurement of Kv7 currents using the whole cell patch clamp technique showed a lower current density in SMCs from coronary compared to those from cerebral arteries (Figure 5 and 7). Secondly, Kv7.4 protein levels were lower in the LAD compared to cerebral vessels suggesting differences in the number of functional channels. Although less likely, a difference in the sensitivity to the Kv7 channel activator between two different cell types, rather than a difference in the absolute number of functional channels, could also contribute to this important observation. Interestingly the BK_{Ca} activator, NS-1619 (30-50 μM) induced similar vasorelaxation in both arteries (Supplementary Figure 2C) suggesting that under basal conditions coronary circulation is more dependent on BK_{Ca} than Kv7 channels. Further supporting this and as noted by Gollasch [37] in the studies of Khanamiri et al. [16], Kv7 blockers (linopirdine and XE991) caused only a very modest reduction in flow (approximately 5-9 % of baseline flow) in isolated perfused heart preparations.

Consistent with other studies, mRNA expression of Kv7.1 was strongly expressed in basilar, Circle of Willis and LAD arteries (see Figure 1 and Supplementary Figure 1C). While some of the reagents used are reported to act on all of Kv7.1-5, the selective Kv7.1 activator, ML277 showed no functional effect either in terms of vasorelaxation or increasing outward K^+ currents in either of the vessel types studied (Supplementary Figure 5). This dissociation between mRNA expression and functional protein has been described by others [15,16] and is suggested to result from the co-expression of an inhibitory subunit [16,30]. This being the case the great majority of Kv7 functional activity in mouse arteries (particularly those of the cerebrovasculature) appears to result from the availability of Kv7.4.

Previous studies have demonstrated, in a range of blood vessel types, the non-selective Kv7 channel inhibitors (Kv7.1 through Kv7.5), linopirdine or XE991 (10 μM) have depolarizing effects on vascular SMCs, which induce vasoconstriction [10,13,14,16,18,35]. In the present study, application of linopirdine or XE991 evoked constriction (10-12% of contraction to 100 mM KCl) in segments of nonpreconstricted cerebral arteries, whereas linopirdine-induced contraction was comparatively blunted in the coronary artery (Figure 3). Consistent with the pharmacological data, we found that linopirdine (10 μM) blocked Kv currents in cerebral artery myocytes, whereas these responses were blunted in coronary artery myocytes (Figure 6 and 7C-D). Further, in the coronary artery myocytes, the Kv7 channel activator retigabine did not increase K^+ currents over the voltage range of -70 mV to +70 mV (Figure 7A and B).

Analysis of the biophysical characteristics of our K^+ current recordings was also undertaken to support the functional and pharmacological approaches. Estimations of E_{Rev} and $V_{1/2}$

showed significant hyperpolarizing effects of retigabine and a depolarizing action of linopirdine on cerebral vessel VSMCs. Similar effects, however, were not observed in VSMCs isolated from LAD. The absolute values obtained in the current studies tended to be at more positive potentials than demonstrated in some other studies [18]. This may, in part, relate to differences in recording protocols and conditions (for example the use of standard whole cell recording versus perforated patch) and variation in the contribution of non-Kv7 channels. Regardless of this, it is clear that differences in the action of known Kv7 channel modulators were detected between cerebral and LAD smooth muscle cells supporting regional heterogeneity in the involvement of this class of K^+ channel.

Recently, Chadha et al. suggested that renal artery Kv7 channels are regulated by cAMP-dependent processes [15]. In the present studies, the cAMP activator, forskolin induced concentration-dependent vasorelaxation in both cerebral and coronary arteries (Figure 4). Forskolin-induced vasorelaxation was attenuated by pre-incubation with 10 μM linopirdine in the cerebral artery, whereas pre-treatment of the same concentration of linopirdine did not alter cAMP-mediated vasorelaxation in the coronary artery, again consistent with Kv7 channels playing a more prominent role in the cerebral than coronary circulation.

Previously, we suggested a more significant role, under basal conditions, for BK_{Ca} in the cerebral vasculature as compared to that of skeletal muscle. While the comparison in this study has been between cerebral and coronary vasculature for the Kv7 family of K^+ channels it is interesting that a similar pattern has been observed. Thus a speculative conclusion is that vasomotor tone is more tightly coupled to K^+ channels (at least in regard to BK_{Ca} and Kv7) in the cerebral vasculature as compared to peripheral tissues. While the various tissues express a number of K^+ channels (including K_{ATP}, intermediate and small conductance K^+ channels and two-pore K^+ channels) and that specific stimuli can modify channel activity through events such as phosphorylation, the studies do suggest differing roles for at least some of the K^+ channels in the different vascular beds.

In summary, the results of these studies demonstrate that Kv7 channels are capable of mediating vasorelaxation in cerebral arteries while being markedly less effective in the coronary circulation. Support for this conclusion was obtained both at the vessel and isolated SMC. Thus, activation of Kv7 channels may be a potentially effective mechanism for selectively increasing cerebral perfusion, and therefore present a potential therapeutic target in patients with cerebrovascular disease including stroke and subarachnoid hemorrhage. Further studies are required to determine exactly why coronary artery Kv7 channel activity is diminished under basal conditions despite their apparent expression at the mRNA level and to understand exactly how this class of channels contributes to the involvement of Kv (in general) in the regulation coronary vascular function [7-9].

Supplementary Material

Refer to Web version on PubMed Central for supplementary material.

Acknowledgements

Thanks are extended to Dr Andrew Braun, University of Calgary, for assisting with analysis of the electrophysiological data and to Dr. Michael J. Davis, University of Missouri, for constructive criticisms of the manuscript prior to submission.

Sources of Funding

This study was supported by grant from NIH grant HL092241.

List of Abbreviations

BK_{Ca}	Large conductance Ca^{2+} activated K^+ channel
Ct	Comparative threshold
DTT	Dithiothreitol
E_{Rev}	Reversal potential
G	Conductance
K_{2p}	Two pore domain K^+ channel
K_{ATP}	ATP-sensitive K^+ channel
K_{ir}	Inward rectifier K^+ channel
Kv	Voltage-gated K^+ channel
LAD	Left anterior descending
PSS	Physiological saline solution
qPCR	Quantitative PCR
SMC	Smooth muscle cell
VSMC	Vascular smooth muscle cell
$V_{1/2}$	Voltage for half maximal activation

References

1. Davis MJ, Hill MA. Signaling mechanisms underlying the vascular myogenic response. Physiol Rev. 1999; 79:387–423. [PubMed: 10221985]
2. Nelson MT, Quayle JM. Physiological roles and properties of potassium channels in arterial smooth muscle. Am J Physiol. 1995; 268:C799–822. [PubMed: 7733230]
3. Korovkina VP, England SK. Detection and implications of potassium channel alterations. Vascul Pharmacol. 2002; 38:3–12. [PubMed: 12378820]
4. Jackson WF. Potassium channels in the peripheral microcirculation. Microcirculation. 2005; 12:113–127. [PubMed: 15804979]
5. Ko EA, Park WS, Firth AL, Kim N, Yuan JX, et al. Pathophysiology of voltage-gated K+ channels in vascular smooth muscle cells: modulation by protein kinases. Prog Biophys Mol Biol. 2010; 103:95–101. [PubMed: 19835907]
6. Jahromi BS, Aihara Y, Ai J, Zhang ZD, Nikitina E, et al. Voltage-gated K+ channel dysfunction in myocytes from a dog model of subarachnoid hemorrhage. J Cereb Blood Flow Metab. 2008; 28:797–811. [PubMed: 17987046]

7. Dick GM, Bratz IN, Borbouse L, Payne GA, Dincer UD, et al. Voltage-dependent K+ channels regulate the duration of reactive hyperemia in the canine coronary circulation. Am J Physiol Heart Circ Physiol. 2008; 294:H2371–2381. [PubMed: 18375717]
8. Berwick ZC, Dick GM, Moberly SP, Kohr MC, Sturek M, et al. Contribution of voltage-dependent K(+) channels to metabolic control of coronary blood flow. J Mol Cell Cardiol. 2012; 52:912–919. [PubMed: 21771599]
9. Berwick ZC, Moberly SP, Kohr MC, Morrical EB, Kurian MM, et al. Contribution of voltage-dependent K+ and Ca2+ channels to coronary pressure-flow autoregulation. Basic Res Cardiol. 2012; 107:264. [PubMed: 22466959]
10. Zhong XZ, Harhun MI, Olesen SP, Ohya S, Moffatt JD, et al. Participation of KCNQ (Kv7) potassium channels in myogenic control of cerebral arterial diameter. J Physiol. 2010; 588:3277–3293. [PubMed: 20624791]
11. Amberg GC, Santana LF. Kv2 channels oppose myogenic constriction of rat cerebral arteries. Am J Physiol Cell Physiol. 2006; 291:C348–356. [PubMed: 16571867]
12. Knot HJ, Nelson MT. Regulation of membrane potential and diameter by voltage-dependent K+ channels in rabbit myogenic cerebral arteries. Am J Physiol. 1995; 269:H348–355. [PubMed: 7631867]
13. Yeung SY, Pucovsky V, Moffatt JD, Saldanha L, Schwake M, et al. Molecular expression and pharmacological identification of a role for K(v)7 channels in murine vascular reactivity. Br J Pharmacol. 2007; 151:758–770. [PubMed: 17519950]
14. Ng FL, Davis AJ, Jepps TA, Harhun MI, Yeung SY, et al. Expression and function of the K+ channel KCNQ genes in human arteries. Br J Pharmacol. 2011; 162:42–53. [PubMed: 20840535]
15. Chadha PS, Zunke F, Zhu HL, Davis AJ, Jepps TA, et al. Reduced KCNQ4-encoded voltage-dependent potassium channel activity underlies impaired beta-adrenoceptor-mediated relaxation of renal arteries in hypertension. Hypertension. 2012; 59:877–884. [PubMed: 22353613]
16. Khanamiri S, Soltysinska E, Jepps TA, Bentzen BH, Chadha PS, et al. Contribution of kv7 channels to Basal coronary flow and active response to ischemia. Hypertension. 2013; 62:1090–1097. [PubMed: 24082059]
17. McCallum LA, Pierce SL, England SK, Greenwood IA, Tribe RM. The contribution of Kv7 channels to pregnant mouse and human myometrial contractility. J Cell Mol Med. 2011; 15:577–586. [PubMed: 20132415]
18. Mani BK, Brueggemann LI, Cribbs LL, Byron KL. Activation of vascular KCNQ (Kv7) potassium channels reverses spasmogen-induced constrictor responses in rat basilar artery. Br J Pharmacol. 2011; 164:237–249. [PubMed: 21323904]
19. Svalo J, Bille M, Parameswaran Theepakaran N, Sheykhzade M, Nordling J, et al. Bladder contractility is modulated by Kv7 channels in pig detrusor. Eur J Pharmacol. 2013; 715:312–320. [PubMed: 23707187]
20. Afeli SA, Malysz J, Petkov GV. Molecular expression and pharmacological evidence for a functional role of kv7 channel subtypes in Guinea pig urinary bladder smooth muscle. PLoS One. 2013; 8:e75875. [PubMed: 24073284]
21. Mulvany MJ, Halpern W. Contractile properties of small arterial resistance vessels in spontaneously hypertensive and normotensive rats. Circ Res. 1977; 41:19–26. [PubMed: 862138]
22. Yang Y, Sohma Y, Nourian Z, Ella SR, Li M, et al. Mechanisms underlying regional differences in the Ca2+ sensitivity of BK(Ca) current in arteriolar smooth muscle. J Physiol. 2013; 591:1277–1293. [PubMed: 23297302]
23. Yang Y, Murphy TV, Ella SR, Grayson TH, Haddock R, et al. Heterogeneity in function of small artery smooth muscle BKCa: involvement of the beta1-subunit. J Physiol. 2009; 587:3025–3044. [PubMed: 19359368]
24. Hamill OP, Marty A, Neher E, Sakmann B, Sigworth FJ. Improved patch-clamp techniques for high-resolution current recording from cells and cell-free membrane patches. Pflugers Arch. 1981; 391:85–100. [PubMed: 6270629]
25. Chang TC, Zeitels LR, Hwang HW, Chivukula RR, Wentzel EA, et al. Lin-28B transactivation is necessary for Myc-mediated let-7 repression and proliferation. Proc Natl Acad Sci U S A. 2009; 106:3384–3389. [PubMed: 19211792]

26. Dettman EJ, Simko SJ, Ayanga B, Carofino BL, Margolin JF, et al. Prdm14 initiates lymphoblastic leukemia after expanding a population of cells resembling common lymphoid progenitors. Oncogene. 2011; 30:2859–2873. [PubMed: 21339739]
27. Lossos IS, Czerwinski DK, Wechser MA, Levy R. Optimization of quantitative real-time RT-PCR parameters for the study of lymphoid malignancies. Leukemia. 2003; 17:789–795. [PubMed: 12682639]
28. Livak KJ, Schmittgen TD. Analysis of relative gene expression data using real-time quantitative PCR and the 2(-Delta Delta C(T)) Method. Methods. 2001; 25:402–408. [PubMed: 11846609]
29. Brueggemann LI, Mackie AR, Cribbs LL, Freda J, Tripathi A, et al. Differential protein kinase C-dependent modulation of Kv7.4 and Kv7.5 subunits of vascular Kv7 channels. J Biol Chem. 2014; 289:2099–2111. [PubMed: 24297175]
30. Chadha PS, Jepps TA, Carr G, Stott JB, Zhu HL, et al. Contribution of kv7.4/kv7.5 heteromers to intrinsic and calcitonin gene-related peptide-induced cerebral reactivity. Arterioscler Thromb Vasc Biol. 2014; 34:887–893. [PubMed: 24558103]
31. Jepps TA, Chadha PS, Davis AJ, Harhun MI, Cockerill GW, et al. Downregulation of Kv7.4 channel activity in primary and secondary hypertension. Circulation. 2011; 124:602–611. [PubMed: 21747056]
32. Chadha PS, Zunke F, Davis AJ, Jepps TA, Linders JT, et al. Pharmacological dissection of K(v)7.1 channels in systemic and pulmonary arteries. Br J Pharmacol. 2012; 166:1377–1387. [PubMed: 22251082]
33. Plane F, Johnson R, Kerr P, Wiehler W, Thorneloe K, et al. Heteromultimeric Kv1 channels contribute to myogenic control of arterial diameter. Circ Res. 2005; 96:216–224. [PubMed: 15618540]
34. Schenzer A, Friedrich T, Pusch M, Saftig P, Jentsch TJ, et al. Molecular determinants of KCNQ (Kv7) K+ channel sensitivity to the anticonvulsant retigabine. J Neurosci. 2005; 25:5051–5060. [PubMed: 15901787]
35. Mani BK, O'Dowd J, Kumar L, Brueggemann LI, Ross M, et al. Vascular KCNQ (Kv7) potassium channels as common signaling intermediates and therapeutic targets in cerebral vasospasm. J Cardiovasc Pharmacol. 2013; 61:51–62. [PubMed: 23107868]
36. Gutman GA, Chandy KG, Grissmer S, Lazdunski M, McKinnon D, et al. International Union of Pharmacology. LIII. Nomenclature and molecular relationships of voltage-gated potassium channels. Pharmacol Rev. 2005; 57:473–508. [PubMed: 16382104]
37. Gollasch M. KCNQ channels and novel insights into coronary perfusion. Hypertension. 2013; 62:1011–1012. [PubMed: 24082053]
38. MJ, C. The Cerebral Circulation. Morgan & Claypool Life Sciences; San Rafael (CA): 2009.
39. Klein LW, Weintraub WS, Agarwal JB, Schneider RM, Seelaus PA, et al. Prognostic significance of severe narrowing of the proximal portion of the left anterior descending coronary artery. Am J Cardiol. 1986; 58:42–46. [PubMed: 3728330]
40. Wuttke TV, Seebohm G, Bail S, Maljevic S, Lerche H. The new anticonvulsant retigabine favors voltage-dependent opening of the Kv7.2 (KCNQ2) channel by binding to its activation gate. Mol Pharmacol. 2005; 67:1009–1017. [PubMed: 15662042]
41. Main MJ, Cryan JE, Dupere JR, Cox B, Clare JJ, et al. Modulation of KCNQ2/3 potassium channels by the novel anticonvulsant retigabine. Mol Pharmacol. 2000; 58:253–262. [PubMed: 10908292]

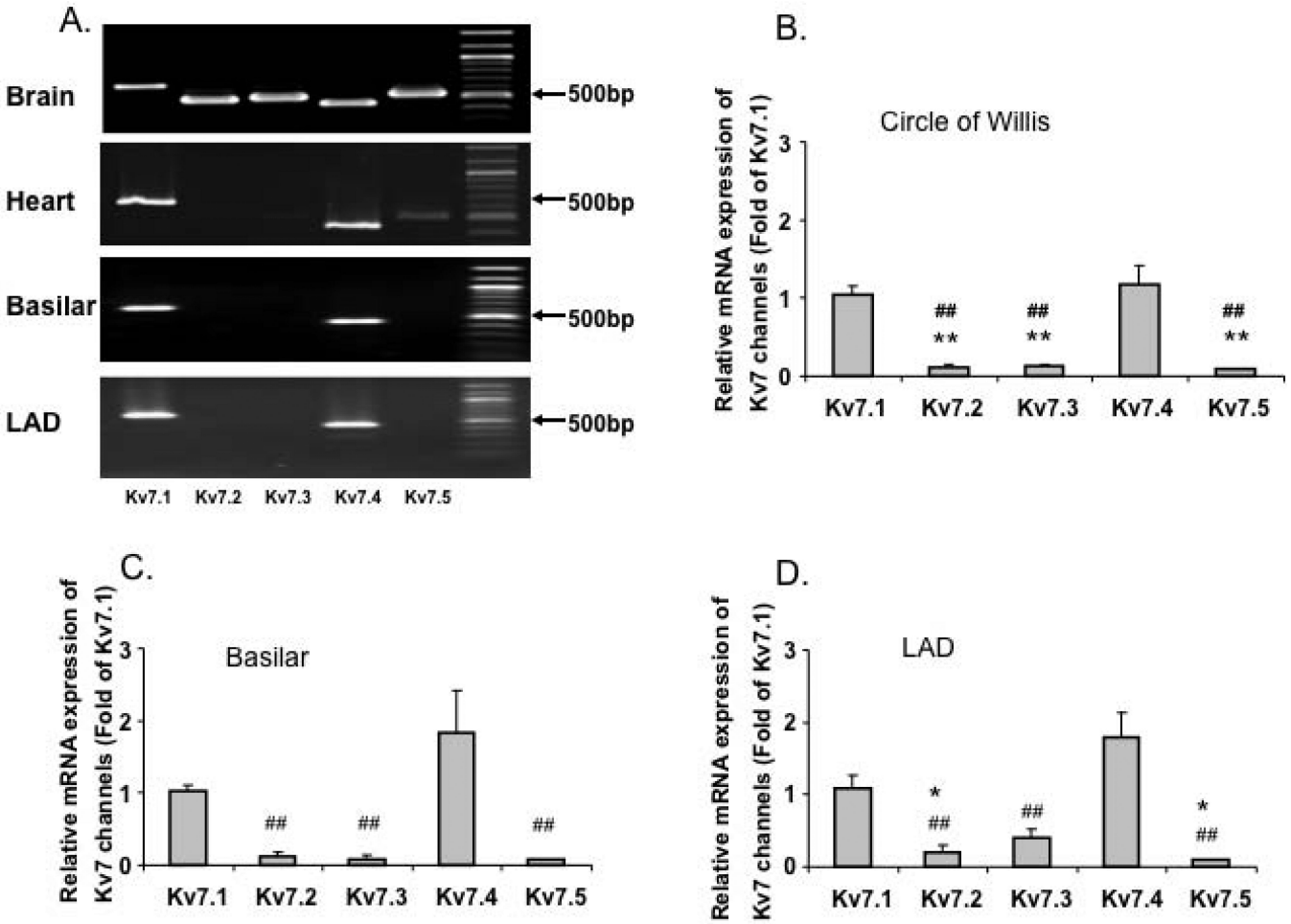

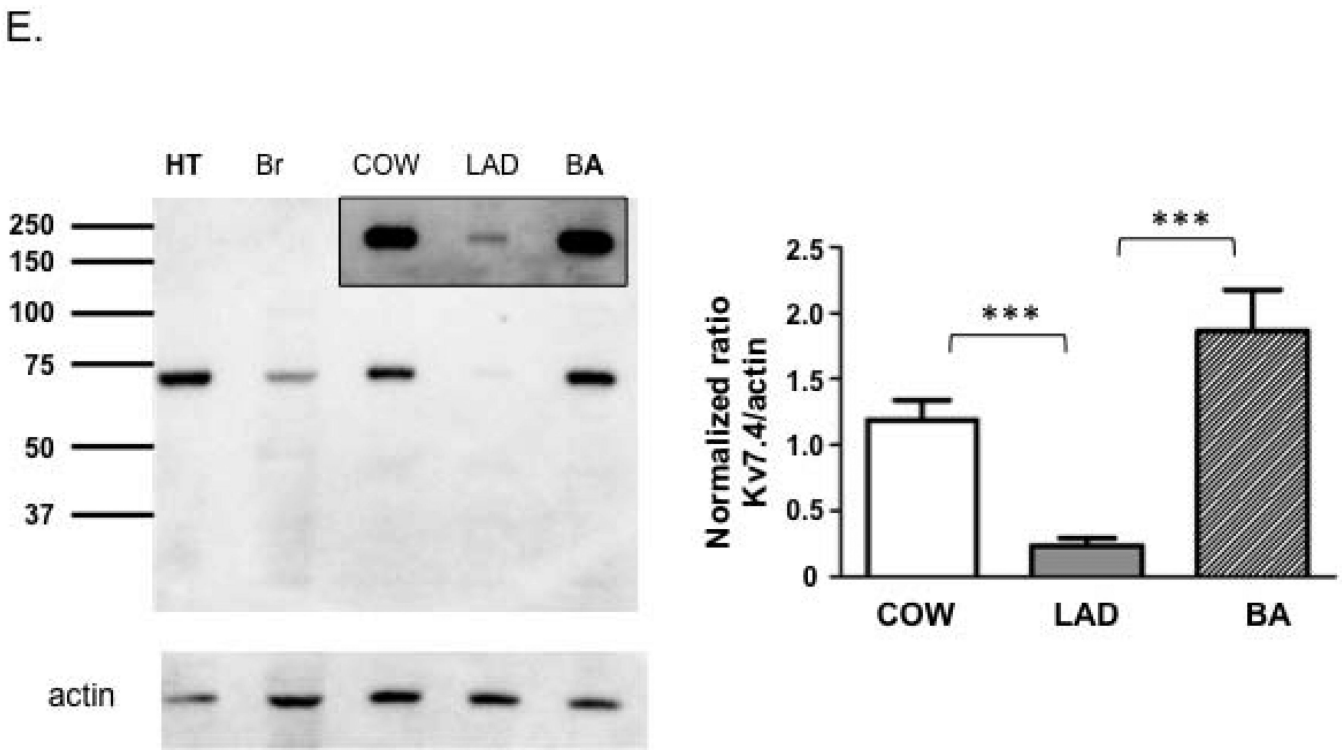

Figure 1. Vascular expression of Kv7 channels

A. End-point PCR analyses of Kv7 channel subtypes in mouse brain, heart, cerebral and coronary arteries. **B, C and D**. Group data for quantitative PCR of Kv7 channel subtypes in mouse Circle of Willis (**B**, n = 5), basilar (**C**, n = 5 - 7) and LAD (**D**, n = 7 - 8) arteries. *P< 0.05, **P<0.01 vs. Kv7.1, ## P<0.01 vs. Kv7.4. **E**, Representative immunoblot for Kv7.4 protein in mouse Circle of Willis cerebral arteries (COW), basilar (BA) and proximal left anterior descending arteries (LAD). Heart (HT) and brain (Br) tissues are included as positive controls. Molecular mass standards are shown in kilo-Daltons. Group data show relative protein levels of Kv7.4 in COW (1.19 ± 0.15, n = 7), LAD (0.24 ± 0.15, n = 7) and BA (1.86 ± 0.32, n = 7). Y-axis is normalized ratio of Kv7.4 band intensity to loading control actin band intensity. Insert shows a longer exposure of the vessel bands to better illustrate the low amount of expression in the small coronary arteries. Results are mean ± SEM. ****P*<0.001 (one-way ANOVA, Bonferroni post-hoc test).

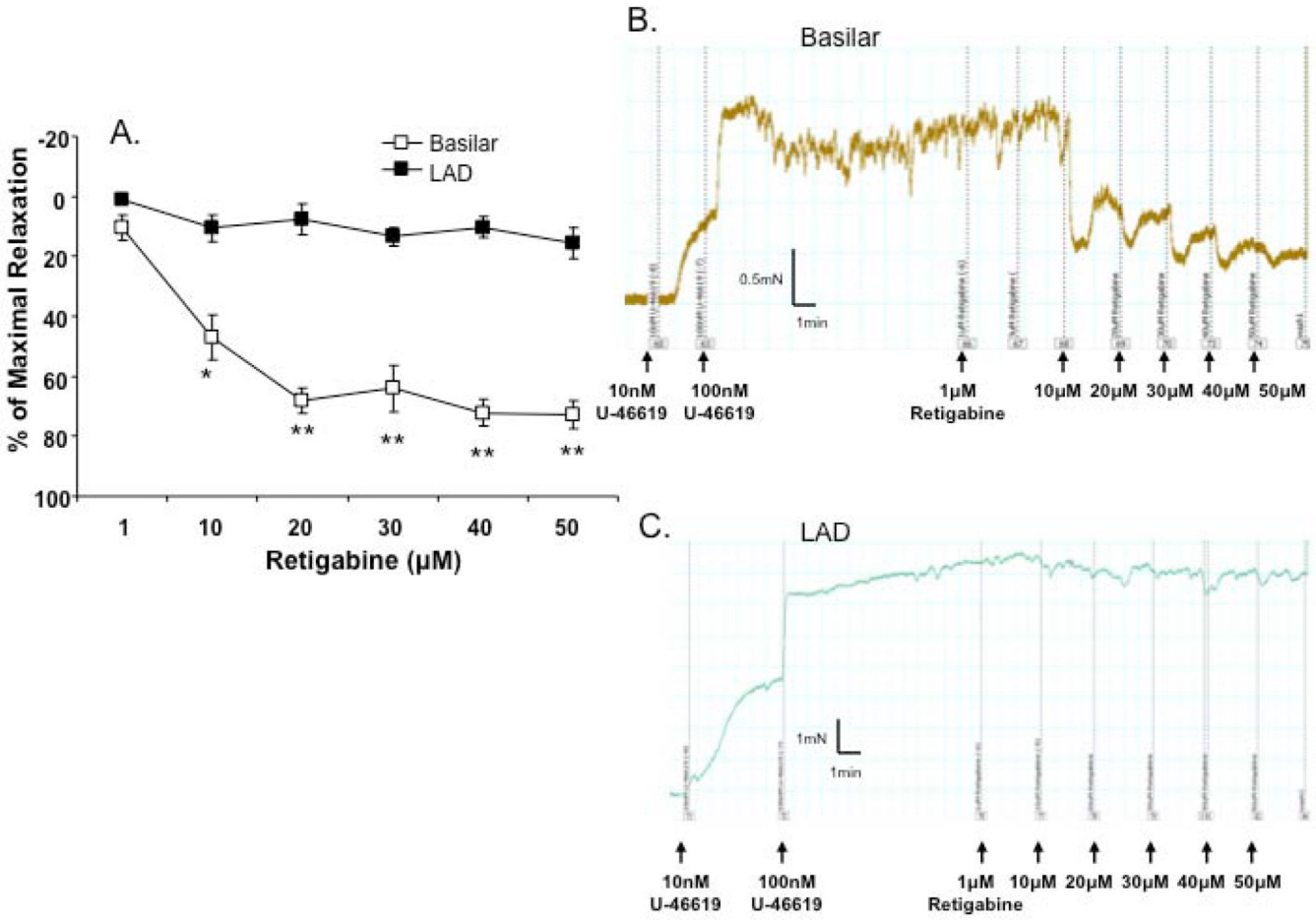

Figure 2. Effect of the Kv7 activator, retigabine on vasorelaxation

A. The Kv7 channel activator, retigabine induced marked vasorelaxation in the basilar (n = 6), while causing slight relaxation in the LAD (n = 6). Data represent the mean ± SEM. *P<0.05, **P<0.01 (two-way, repeated measures, ANOVA, Bonferroni post-hoc test). **B and C.** Representative traces showing concentration-dependent relaxation to retigabine in cerebral (**B**. basilar) and coronary (**C**. LAD) arteries pre-contracted with 100 nM U-46619.

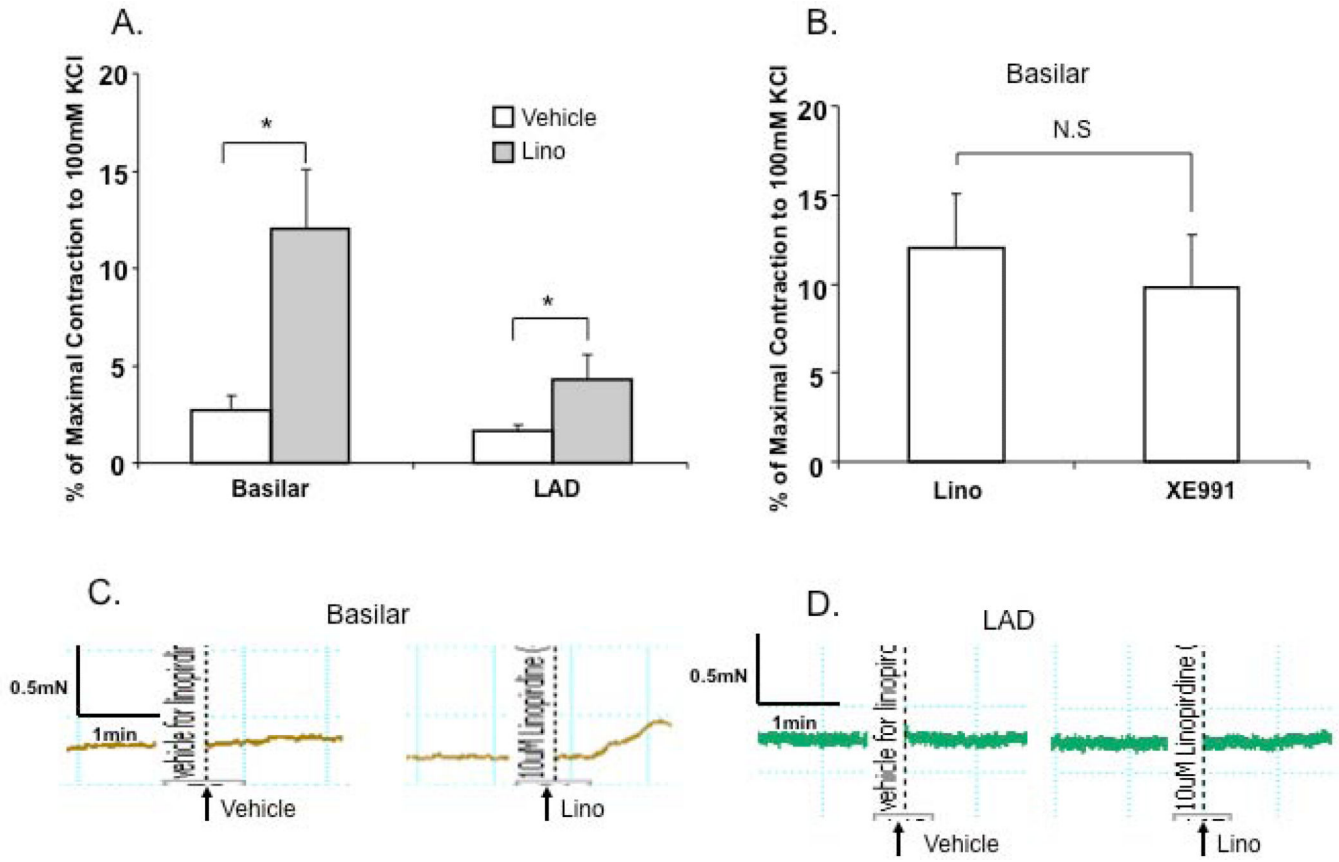

Figure 3. Effects of non-selective Kv7 channel blockers, linopirdine (Lino) and XE991 in coronary and cerebral vasculatures

A. Maximal contractile responses in the presence of 10 μM linopirdine vs. vehicle (ethanol) in isolated coronary and cerebral arteries (n=6). *P<0.05 vs. vehicle (Student-t test). **B**. Maximal contractile responses to linopirdine (10 μM, n = 6) or XE991 (10 μM, n = 4) in basilar arteries. **C and D**. Representative traces showing responses to 10 μM linopirdine vs. vehicle (ethanol) in isolated basilar (C) and LAD (D) arteries.

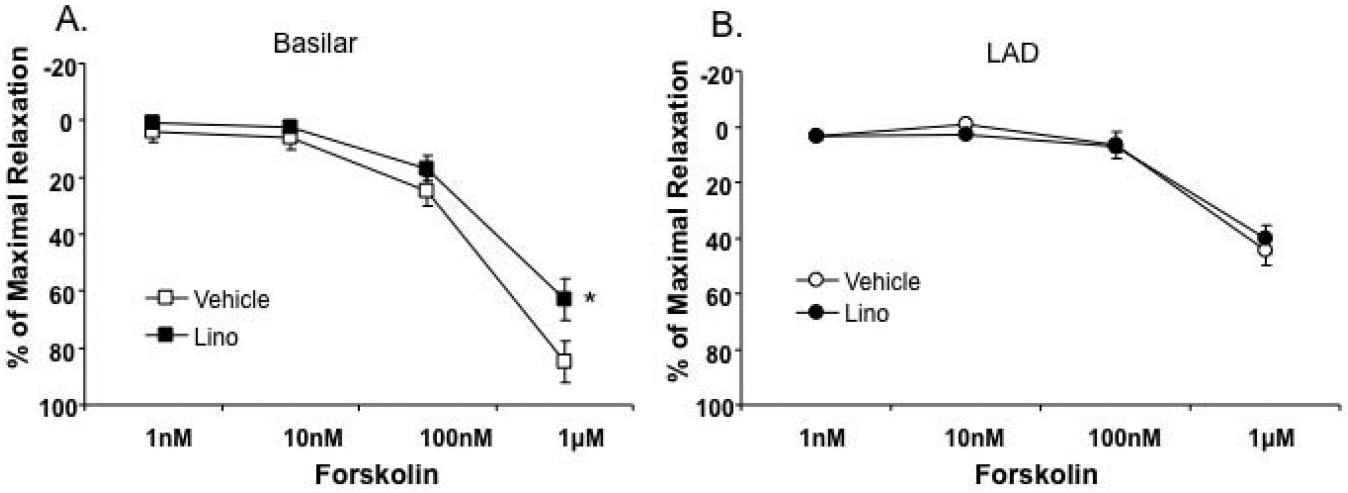

Figure 4. Differing contributions of Kv7 channels in cAMP-mediated vasorelaxation between cerebral and coronary arteries

Concentration-dependent relaxation to forskolin (1 nM – 1 μM) was, in part, inhibited by 10 μM linopirdine (Lino) in basilar arteries (**A**, n = 6), but not in LAD (**B**, n = 6). 2 way, repeated measures, ANOVA with Bonferroni multiple comparisons post hoc test; *P<0.05 vs. vehicle.

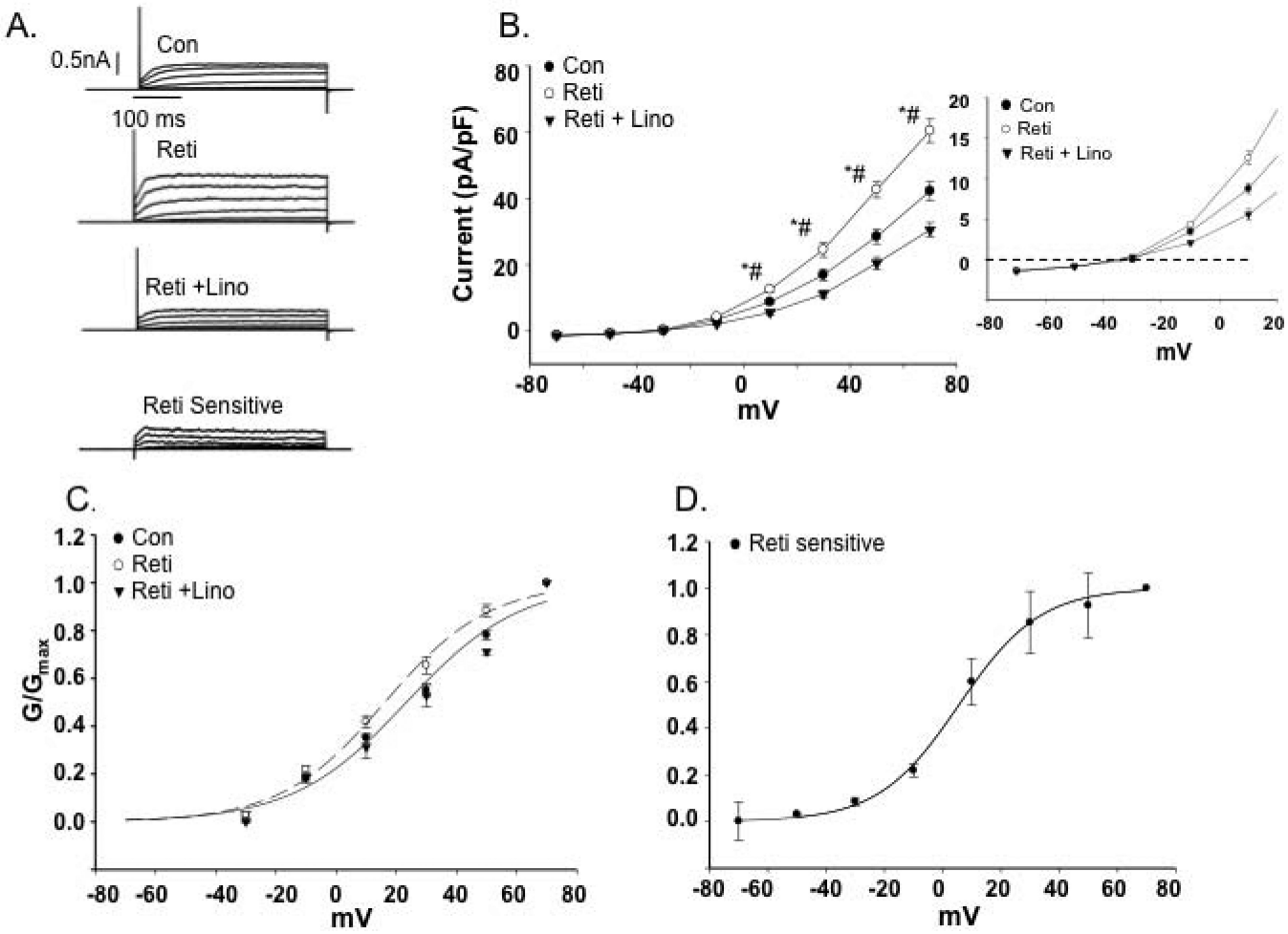

Figure 5. Effects of Kv7 channel modulators on cerebral artery SMC outward K^+ currents

A. Representative traces of outward K^+ currents in cerebral artery VSMCs evoked by steps (300 ms) to voltages over the range -70 to +70 mV with an initial holding potential of -70 mV. The Kv7 channel activator, retigabine (Reti, 20 μM) increased K^+ currents but was inhibited by application of the inhibitor, linopirdine (Lino, 10 μM). **B.** Group I-V curves show that retigabine increases K^+ currents while linopirdine after retigabine decreases K^+ currents in a voltage dependent manner (n = 6 mice, 22 cells). Insert shows a limited voltage range highlighting inward current at negative potentials (for E_{Rev} values see Table 3). 2 way, repeated measures, ANOVA with Bonferroni multiple comparisons post hoc test ; *P< 0.05 vs. Con, # P<0.05 vs. retigabine. **C.** Normalized conductance plotted as a function of voltage. Curve fitting was performed using a Boltzmann function; $V_{1/2}$ values are shown in Table 3. **D.** Retigabine-sensitive K^+ current calculated by subtraction of currents recorded in the absence and presence of retigabine. $V_{1/2}$ values for panels C and D are shown in Table 3.

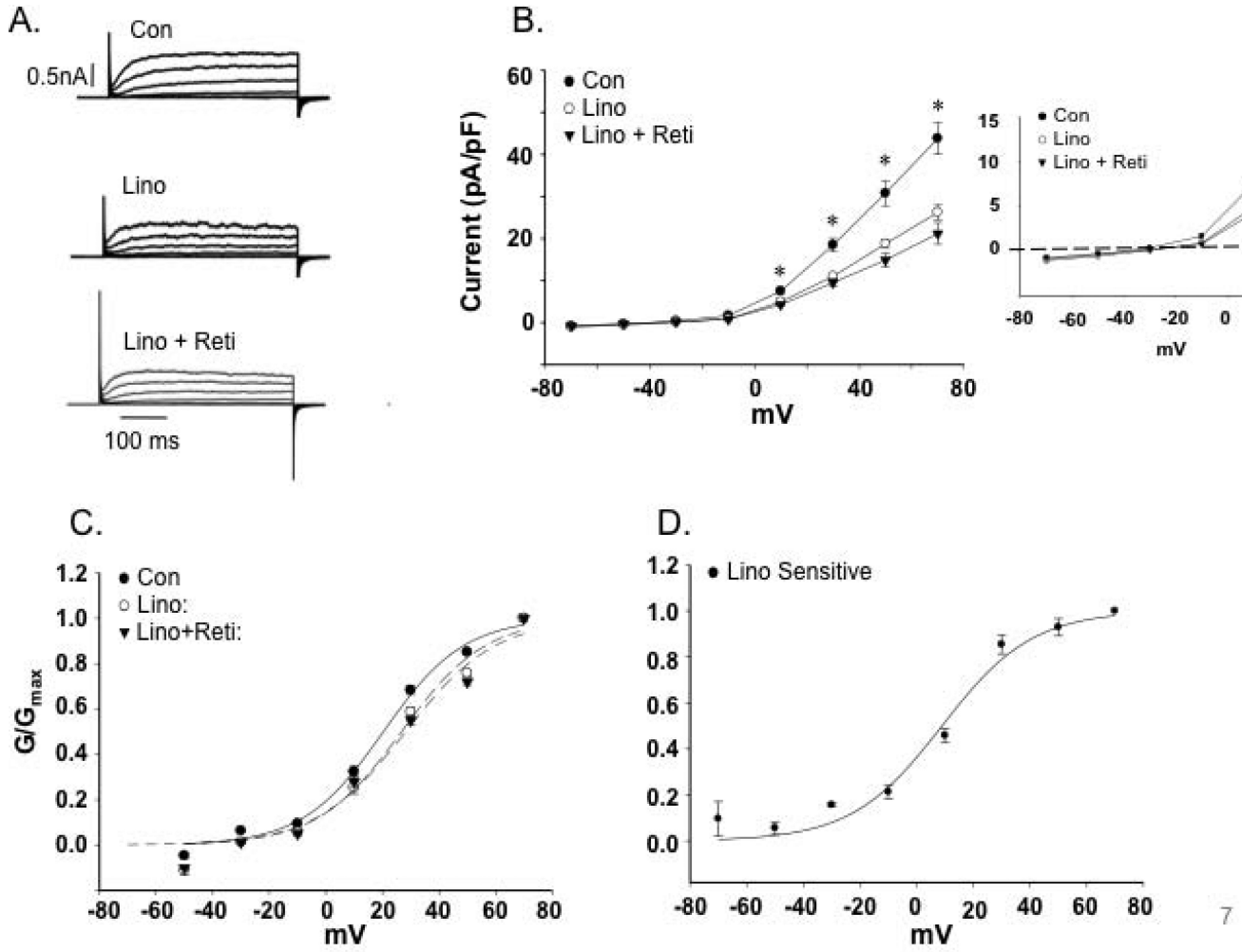

Figure 6. Effects of the Kv7 channel inhibitor, linopirdine (Lino) on the cerebral artery SMC K^+ currents

A. Representative traces of outward K^+ currents in cerebral artery VSMCs evoked by steps (300 ms) to voltages over the range -70 to +70 mV with an initial holding potential of -70 mV. The Kv7 channel inhibitor, linopridine (10 μM) decreased K^+ currents; an effect not reversed by sequential application of retigabine (20 μM). **B.** Group I-V curves showing linopirdine decreases K^+ currents (n = 6 mice, 22 cells). Insert shows a limited voltage range highlighting inward current at negative potentials (for E_{Rev} values see Table 3). 2 way, repeated measures, ANOVA with Bonferroni multiple comparisons post hoc test; *P< 0.05 compared to control. **C.** Normalized conductance plotted as a function of voltage. Curve fitting was performed using a Boltzmann function; $V_{1/2}$ values are shown in Table 3. **D.** Linopirdine-sensitive K^+ current calculated by subtraction of currents recorded in the absence and presence of linopirdine. $V_{1/2}$ values for panels C and D are shown in Table 3.

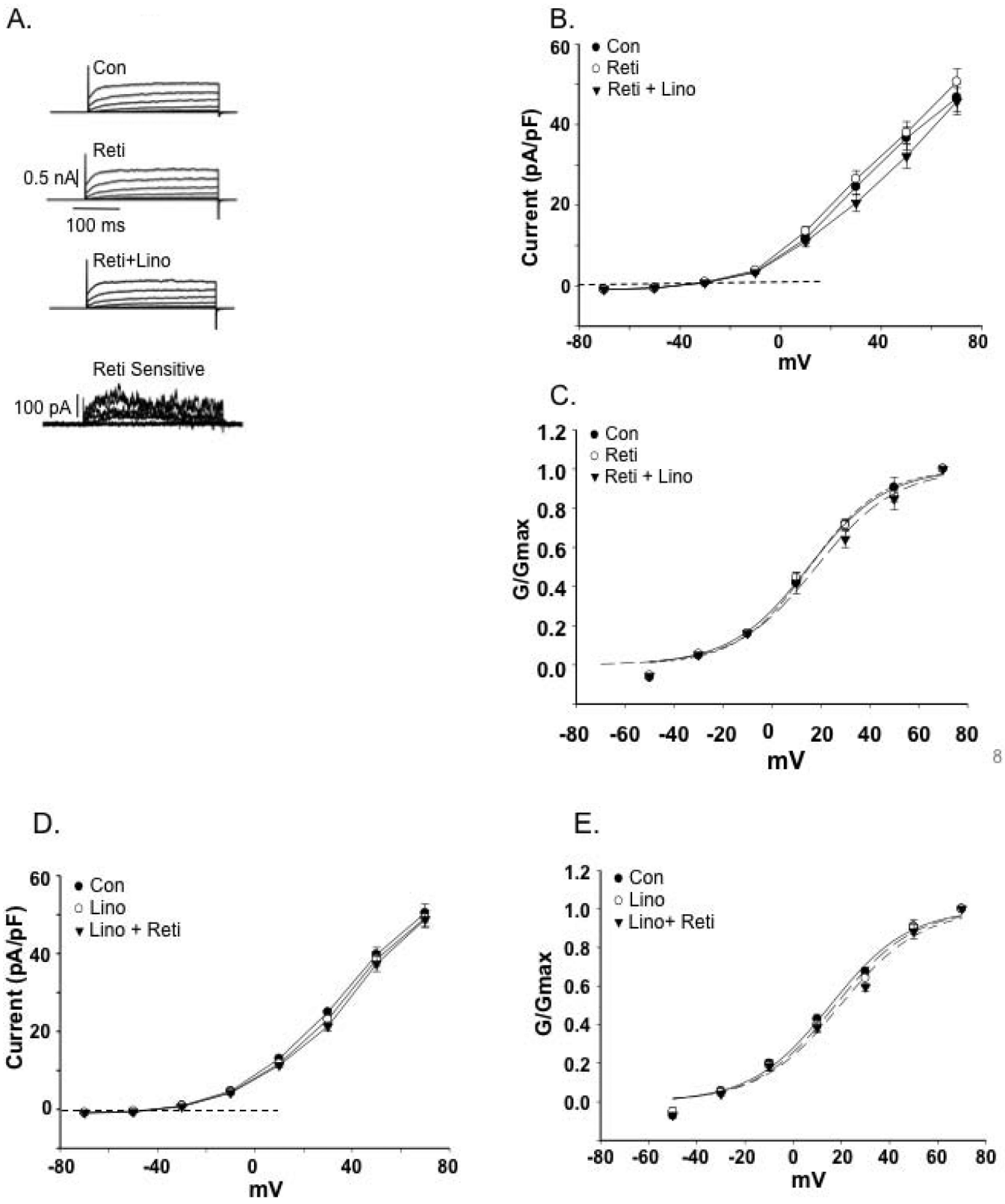

Figure 7. Effects of Kv7 channel modulators on coronary artery SMC K^+ currents

A. Representative traces of outward K^+ currents in LAD VSMCs evoked by steps (300 ms) to voltages over the range -70 to +70 mV with an initial holding potential of -70 mV. As highlighted by the retigabine-sensitive component a minimal increase in current was observed on application of the activator. **B**. Group I-V curves showing the effects of retigabine (Reti) and sequential addition of linopirdine (Lino) on K^+ currents in LAD VSMCs (n = 5 mice, 20 cells). **C.** Normalized conductance plotted as a function of voltage. Curve fitting was performed using a Boltzmann function; $V_{1/2}$ values are shown in Table 3. **D.** Group I-V curves showing minimal effects of linopirdine on Kv7 currents under basal conditions. **E.** Normalized conductance plotted as a function of voltage. Curve fitting was performed using a Boltzmann function; $V_{1/2}$ values are shown in Table 3.

Table1

Primer Sequences used for End-point PCR

Gene Name	Accession#	Strand	Sequence	Amplicon
Kcnql	NM_008434			
		s	TTGTGGTGTTCTTTGGGACA	647
		as	TGCAGTCTGGATGAGTGAGG	
Kcnq2	NM_010611			
		s	TCTCCTGCCTTGTGCTTTCT	490
		as	GCATCTGCGTAGGTGTCAAA	
Kcnq3	NM_152923			
		s	ATCGGGTTCGCCTTTCTAAT	509
		as	CTGCTGGGATGGGTAGGTAA	
Kcnq4	NM_001081142			
		s	GCTTACGGTGGATGATGTCA	449
		as	TGTGGTAGTCCGAGGTGATG	
Kcnq5	NM_023872			
		s	GGCTTCGCACTCCTTGGCAT	535
		as	CACACTGGCATCCTTTCTCA	

Table2

Primer Sequences used for qPCR

Gene Name	Accession#	Strand	Sequence	Amplicon (bp)	Amplification
Kcnql	NM_008434				
		s	TTC GCC ACA TCA GCT ATC AG	141	2.02
		as	AAT GTA CAG GGT GGT GAT CAG		
Kcnq2	NM_010611				
		s	GTT CAT CTA CCA CGC CTA CG	140	1.98
		as	CAC CGA ATA CCA CGA TAG TCA C		
Kcnq3	NM_152923				
		s	GTC AGC ATT TAC CTA CCC ATC C	148	1.94
		as	GTC CAG TTT CTT CCC CAT GTC		
Kcnq4	NM_001081142				
		s	GGA GGC AGT GGA TGA AAT CAG	101	1.92
		as	AGT AGA AGC CCA GCA GCA		
Kcnq5	NM_023872				
		s	TCATCCTTCCTTGTCTATCTTGTG	140	1.99
		as	AGTCTTCCCAGCCACGTTA		
Rn18s	NR_003278	s	GTAACCCGTTGAACCCCATT	151	1.92
		as	CCATCCAATCGGTAGTAGCG		

TABLE 3

Biophysical Parameters for Cerebral and LAD VSMCs

	E_{Rev}	$V_{1/2}$
Cerebral VSMCs		
Control	−33.9 ± 1.3	23.3 ± 1.9
+ Retigabine	−37.4 ± 1.2*	16.2 ± 1.8*
Retigabine sensitive#		6.7 ± 0.9
Control	−36.9 ± 1.1	20.7 ± 1.1
+ Linopirdine	−32.2 ± 1.4*	26.4 ± 1.4*
Linopirdine sensitive#		8.9 ± 2.7
LAD SMCs		
Control	−35.5 ± 2.3	15.6 ± 1.7
+ Retigabine	−37.3 ± 2.5	15.1 ± 1.3
Control	−38.7 ± 1.3	15.5 ± 1.6
+ Linopirdine	−37.7 ± 2.1	17.5 ± 2.2

sensitive components calculated by subtraction of control data and that obtained in the presence or either retigabine or linopirdine

* $p < 0.05$ compared to control recording (paired t-test)